Available online at www.sciencedirect.com
SCIENCE DIRECT
Thermochimica Acta 434 (2005) 93–99
thermochimica acta
www.elsevier.com/locate/tca

# Microcalorimetry, TPR and XPS studies of acid–base properties of NiCuMgAl mixed oxides using LDHs as precursors

L. Dussault[a], J.C. Dupin[a], E. Dumitriu[b], A. Auroux[c], C. Guimon[a,*]

[a] *LCTPCM, UMR 5624-FR 2606-CNRS, Université de Pau, Hélioparc Pau Pyrénées, 2 av du Président Angot, 64053 Pau Cedex 9, France*
[b] *Laboratory of Catalysis, Technical University of Iasi, 71 D. Mangeron Avenue, 700050 Iasi, Romania*
[c] *IRC, 2 avenue A. Einstein, 69626 Villeurbanne Cedex, France*

Received 26 August 2004; received in revised form 17 November 2004; accepted 5 January 2005
Available online 10 February 2005

**Abstract**

NiCuMgAl layered double hydroxides (LDHs) with hydrotalcite-like structure containing different proportions of $Ni^{2+}$, $Cu^{2+}$, $Mg^{2+}$ and $Al^{3+}$ cations have been prepared. Thermogravimetry and X-ray diffraction data indicate that the transformation of LDH into mixed oxides is effective after calcination at 450 °C. The acid–base properties of these mixed oxides have been investigated using adsorption microcalorimetry and X-ray photoelectron spectroscopy with $SO_2$ (for basicity) and $NH_3$ (for acidity) as probe molecules.

The basicity depends principally on the Ni/Cu ratio and increases with the Ni proportion. The strength (strong and medium) of the basic sites is particularly homogeneous. On the surface of the oxides, they are both Brönsted (∼60%) and Lewis sites (∼40%).

The acidity (only Lewis type) is rather weak and dependant, as the basicity, of the Ni/Cu ratio. The observed heterogeneity of these sites can be related to the heterogeneity of the interactions between the nickel atoms and the other elements.


*Keywords:* NiCuMgAl mixed oxides; Layered double hydroxides; Acidity; Basicity; Microcalorimetry; XPS; TPR

## 1. Introduction

Layered double hydroxides (LDHs) or hydrotalcite-like compounds have the general formula $[M_{1-x}^{2+}M_x^{3+}(OH)_2]^{x+}(A^{n-})_{x/n}\cdot yH_2O$ and belong to the class of anionic clays [1]. The identities of the di- and trivalent cations ($M^{II}$ and $M^{III}$) and the interlayer anion ($A^{n-}$) together with the value of the stoichiometric coefficient ($x$) may be varied over a wide range, giving rise to a large class of isostructural materials. Their structure consists of positively charged brucite-like layers. When part of $Mg^{2+}$ from the brucite layers ($Mg(OH)_2$) is substituted by a trivalent cation, a formal positive charge appears in hydroxyl layers which is counterbalanced by exchangeable anions $A^{n-}$ located, as water molecules, in the interlayer space.

Thermal treatments of LDHs induce dehydration, dehydroxylation and loss of compensating anions, and give a stable, high surface area, homogeneous and highly dispersed mixed metal oxides with acidic, basic and redox characteristics [1,2]. LDHs, either as such or after thermal decomposition, have found a wide variety of uses as anions exchangers, adsorbents, catalysts and catalyst supports. The activity of these catalysts, related to their acid–base and/or redox properties (when they contain a reducible metal), depends on their composition, the preparation method and the treatment conditions.

In this paper, we examine the thermal decomposition of MgNiCuAl LDHs (with $CO_3^-$ as interlayer anions) by XRD, TPR, TGA and X-ray photoelectron spectroscopy (XPS). In a second stage, we determine the evolution of the surface acido-basicity of the corresponding mixed oxides obtained by calcination at 723 K with the help of adsorption microcalorimetry and adsorption XPS.

* Corresponding author. Tel.: +33 559 407 620; fax: +33 559 407 622.
*E-mail address:* claude.guimon@univ-pau.fr (C. Guimon).

0040-6031/$ – see front matter © 2005 Elsevier B.V. All rights reserved.
doi:10.1016/j.tca.2005.01.012

## 2. Experimental

### 2.1. Materials

Eight LDH samples with different Ni/Cu/Mg/Al compositions (Table 1) were prepared by co-precipitation method. An aqueous solution containing appropriate amounts of $Mg(NO_3)_2{\cdot}6H_2O$, $Al(NO_3)_3{\cdot}9H_2O$, $Cu(NO_3)_2{\cdot}3H_2O$ and $Ni(NO_3)_2{\cdot}6H_2O$ was added dropwise to a vigorously stirred solution containing a slight excess of $Na_2CO_3$. The pH was maintained constant ($9.5 \pm 0.2$) by NaOH addition. Precipitate was kept in suspension at 75 °C for 15 h under stirring. The resulting solid was filtered, thoroughly washed with distilled water and dried overnight at 80 °C.

The samples are named according to their formal composition, i.e. the relative proportions of the metals (Ni/Cu/Mg/Al, 0/1/1/1, 0.2/0.8/1/1, etc.). The real compositions, determined by ICP AES, are very close to these ones. In this series, we varied, on the one hand, the Cu/(Cu + Ni) ratio (with Mg/Al constant) and, on the other hand, the Mg/Al ratio (with Cu/(Cu + Ni) constant). After calcination, except the sample without nickel (0/1/1/1), the BET surface areas (Table 1) lie between 209 and 316 $m^2\ g^{-1}$.

### 2.2. Characterisation

The X-ray diffraction (XRD) patterns of LDHs and corresponding mixed oxides formed by their thermal decomposition were recorded using a INEL diffractometer using a curved position-sensitive detector (INEL CPS 120) calibrated with $Na_2Ca_3Al_2F_{14}$ as standard. The monochromatised radiation applied was Cu Kα (1.5406 Å) from a long fine focus Cu tube operating at 40 kV and 20 mA. Scans were performed over the $2\theta$ range from 10° to 90°.

Thermogravimetric experiments were carried out on a TGA model 2950 coupled with a Mass Spectrometer (TA Instruments) from 30 to 850 °C (5 °C $min^{-1}$) under nitrogen flow.

The XPS analyses were carried out with a Kratos spectrometer (model Axis Ultra) using a focused monochromatised Al Kα radiation (1486.6 eV) under a residual pressure of $10^{-7}$ Pa. To prevent any exposure of the sample to air after $NH_3$ and $SO_2$ adsorption and before analysis, the XPS spectrometer was directly coupled to a glove box. The hemispherical analyser functioned with a constant pass energy of 40 eV for high-resolution spectra. The analysed area of the samples was 300 μm × 700 μm. Charge neutralisation was used for all measurements to compensate the charge effects. The binding energy scale was calibrated using the Al 2p peak at 75.0 eV (corresponding to $Al(OH)_3$) for precursors and at 74.1 eV (corresponding to $Al_2O_3$) for calcined samples. The XPS signals were analysed using a nonlinear Shirley-type background [3]. The fitting peaks of the experimental curves were calculated using a combination of Gaussian (70%) and Lorentzian (30%) functions. For the deconvolution of the S 2p bands (S $2p^{3/2}$–S $2p^{1/2}$ doublet), the theoretical peaks were obtained using fixed intensity ratio ($2p^{3/2}/2p^{1/2} = 2$), fixed spin-orbit split (1.2 eV) and fixed FWHM (full-width at half-maximum: 1.9 eV) deduced from the spectra of reference compounds. A minimum number of doublets have always been used in the fitting of the experimental curves.

Temperature-programmed reduction (TPR) measurements of the samples were carried out in a quartz reactor of a flow system (GIRA, X-sorb model) equipped with a TCD (thermal conductivity detector). Prior to the TPR experiments, the precursors were calcined at 450 °C under argon flow with linear heating rate (1 °C $min^{-1}$). The TPR runs were carried out with linear heating rate ($\beta = 4$ °C $min^{-1}$) in a temperature range of 30–800 °C. A hydrogen–argon mixture (5–95%) was used to reduce the sample (100 mg) at a flow rate of 20 ml $min^{-1}$. The experimental $H_2$ consumption was monitored on line by a calibration carried out by a pure argon circulation with the same flow.

Microcalorimetric measurements of ammonia and sulfur dioxide adsorption were carried out at 80 °C using a Tian-Calvet-type apparatus (C80 from Setaram). The apparatus was linked to a volumetric line allowing the introduction of reactive gaseous probes. The equilibrium pressure after the introduction of each gas dose was measured by means of a differential pressure gauge from Datametrics. Successive doses were sent onto the sample until a final equilibrium pressure of 67 Pa was obtained. Before adsorption, samples were outgassed at 400 °C overnight. The adsorption was performed at 80 °C to limit physisorption. The amount of intermediate and strong sites was evaluated from the difference between the primary and the secondary isotherms obtained after desorption under secondary vacuum at 80 °C and re-adsorption of the gas under an equilibrium pressure of 27 Pa. This difference is named irreversibly chemisorbed amount ($V_{irr}$).

Table 1
Molar proportions of synthesised LDHs and BET areas of corresponding mixed oxides

| Composition | Cu/(Cu + Ni) | Mg/Al | $M^{II}/M^{III}$ | BET ($m^2\ g^{-1}$) |
|---|---|---|---|---|
| 0/1/1/1 | 1 | 1 | 2 | 108 |
| 0.2/0.8/1/1 | 0.8 | 1 | 2 | 232 |
| 0.8/0.2/1/1 | 0.2 | 1 | 2 | 316 |
| 0.9/0.1/1/1 | 0.1 | 1 | 2 | 272 |
| 0.4/0.1/1/2 | 0.2 | 0.5 | 0.75 | 289 |
| 0.4/0.1/1.5/2 | 0.2 | 0.75 | 1 | 295 |
| 0.4/0.1/1/1 | 0.2 | 1 | 1.5 | 284 |
| 0.4/0.1/1.5/1 | 0.2 | 1.5 | 2 | 209 |

## 3. Results and discussion

### 3.1. Physicochemical characterisation

Fig. 1 shows examples of X-ray diffractograms of dried and calcined LDHs. The XRD pattern for this representative sample reveals an hexagonal structure with sharp symmetric peaks for the (0 0 3), (0 0 6), (1 1 0) and (1 1 3) planes

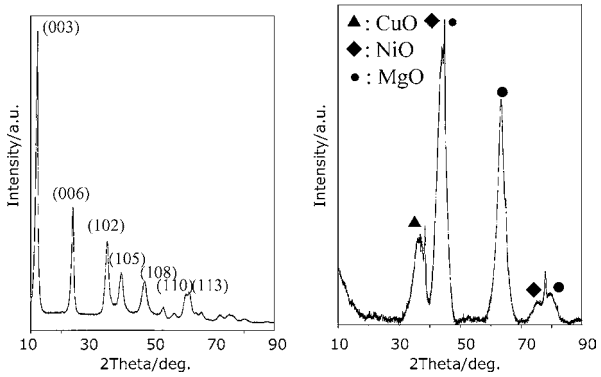


Fig. 1. XRD patterns of as-synthesised and calcined (450 °C) NiCuMgAl (0.8/0.2/1/1) LDH.

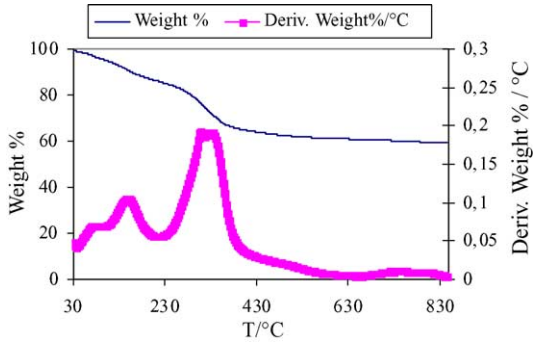


Fig. 2. TG/DTG analysis of NiCuMgAl (0.8/0.2/1/1) LDH.

and broad and asymmetric reflections for (1 0 2), (1 0 5) and (1 0 8) planes, characteristic of hydrotalcite-like compounds [4]. The XRD pattern of 0.8/0.2/1/1 (Fig. 1) shows two peaks with a low intensity between 50° and 60° which have already been observed in well-crystallised hydrotalcites. These diffraction peaks could come from a little part of magnesium hydroxide not included in the brucite structure.

The crystallographic parameters ($a$ and $c$) of LDH samples were calculated for an hexagonal cell on the basis of rhombohedral $R3m$ space group (1 6 6). The parameter $a$ is given by the formula $a = 2d_{110}$ (with respect to hexagonal axes) and $c = 3c'$ ($c'$ is the thickness of one layer constituted by a brucite-like sheet and one interlayer). As indicated by the XRD pattern, no excess phase was detected, so we can conclude that $Ni^{2+}$ and $Cu^{2+}$ have isomorphically replaced the $Mg^{2+}$ cations in the brucite layer. The lattice parameters $a$ and $c$ were calculated using the lattice distances $d_{003}$ and $d_{110}$ ($a = 2d_{110} = 3.05362$ Å and $c = 3d_{003} = 22.76493$ Å). The values are close to those of the literature for this type of material [4].

The calcination of the samples was made under a flow of inert gas (helium) with a rate of 5 °C $min^{-1}$ up to 450 °C (2 h) and then analysed by XRD.

The spectrum of the calcined sample shows only a series of broad peaks corresponding to reflections close to those of MgO (JCPDS file no. 78-0430), NiO (JCPDS file no.78-0643) and CuO (JCPDS file no. 80-1916) in agreement with the literature [5–8]. Thus the calcination of the sample causes dehydroxylation and a loss of the charge compensating anions and leads to the conversion of the LDH to an amorphous homogeneous oxide mixture.

A thermogravimetric study was performed to confirm these results. An example of the TG/DTG curves (mass losses as a function of temperature and the corresponding differential curves) is shown in Fig. 2. The total mass loss is in the range 30–35% for all the samples and is practically effective above 450 °C as for NiMgAl [9] and CuMgAl LDHs [10].

The first mass loss at low temperature (<100 °C) corresponds to the removal of physisorbed water on the surface of material. The second mass loss (around 150 °C) corresponds to the interlayer water. The third loss, at about 300 °C, is caused by the removal of the compensating anions, carbonates ions in our case, and of the water from the dehydroxylation of the brucite layers. The mass loss varies according to the composition of the sample. It is noticed that the temperatures of dehydroxylation are lower for the Cu-rich samples.

The temperature-programmed reduction data of three samples 0/1/1/1, 0.2/0.8/1/1 and 0.8/0.2/1/1 are shown in Fig. 3. With the gradual replacement of copper for nickel, different peaks can be identified. The first peak of each curve below 300 °C is associated to the reduction of the copper ($Cu^{II} \rightarrow Cu^0$) [11]. Only one peak is observed in this region for the CuMgAl (0/1/1/1) mixed oxide. It comes from the

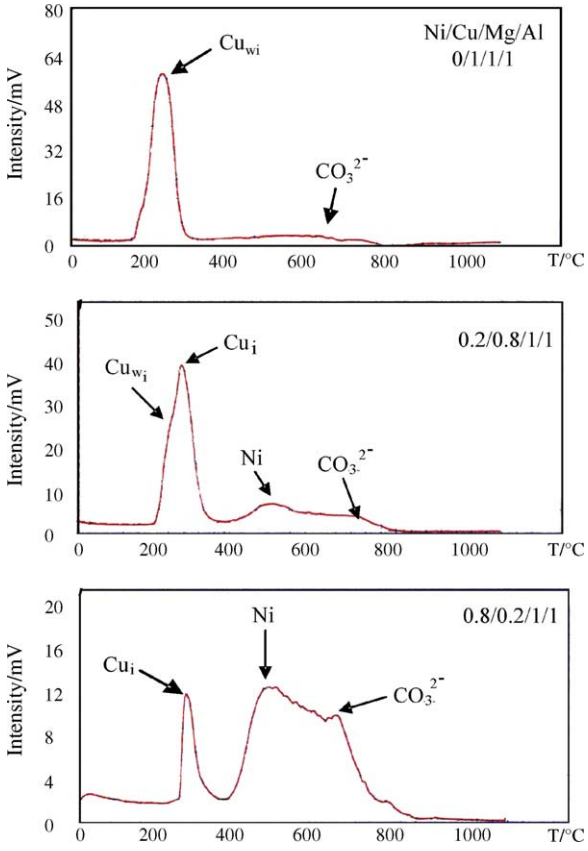


Fig. 3. TPR patterns of NiCuMgAl mixed oxides.

reduction of the highly dispersed copper oxide. The shape and the maximum (240 °C) of this peak are characteristic of the reduction of copper without (or very weak; labelled $Cu_{wi}$ in Fig. 3) interaction with the support. Indeed, the reduction temperature is very close to that of pure CuO (with crystallite size about 14 nm) at 230 °C [12].

The presence of nickel in the composition induces a shift of the maximum (280 °C) of this peak. In 0.2/0.8/1/1 oxide, the preceding peak at 240 °C (Cu without interaction) appears as a shoulder of the main peak which should be assigned to the reduction of the copper atoms in interaction with the nickel atoms (labelled $Cu_i$ in Fig. 3). This shift toward the high temperatures indicates a small charge transfer in opposite direction than that observed for example in Cu–Zn system [12] and could be related to the respective electronegativities of these different elements.

When the Ni/Cu ratio increases (0.8/0.2/1/1), the low-temperature shoulder disappears. The quite sharp peak at 280 °C indicates that all the copper atoms are in homogeneous interaction with nickel atoms. This confirms thus our hypothesis about this type of interaction between the reducible metals.

At high temperature, the TPR spectra show a broad band with two maxima, the first at about 500 °C, the second around 700 °C. The first peak between 450 and 600 °C is asymmetric and characteristic of Ni with different interactions with the other elements [13]. This agrees the observations of Forsanari et al. [4] for the NiMgAl mixed oxides. In this case, the authors concluded that the decrease in reducibility of $Ni^{2+}$ ions may be attributed to the presence of foreign ions ($Mg^{2+}$ or/and $Al^{3+}$) in NiO phase. The reduction of pure black NiO occurs below 420 °C [14–16], whereas NiO in interaction with alumine support is reduced between 500 and 600 °C [17] and nickel aluminate above 700 °C [18]. As shown by the XRD spectra and in agreement with the literature, aluminates are not generated in our calcination conditions (the spinel phase is only observed after calcination at or above 800 °C). Thus the TPR data show an heterogeneity of the interactions between the nickel atoms and the other metallic elements (Cu, Mg, Al), contrary to the copper atoms which seems to interact with alone Ni.

Moreover, the reduction of residual carbonates is observed ~700 °C), despite the calcination at 450 °C, in agreement with preceding studies [9,10]. In Table 2 we report the XPS $CO_3^-$/Al ratio for the sample NiCuMgAl 0.8/0.2/1/1 taken as example, after synthesis (LDH), after calcination at 450 and 800 °C and after reduction at 700 °C. For LDH, this ratio is slightly lower than the expected value (0.4 instead of 0.5) because of the ultra-high-vacuum conditions of the XPS analysis. A small part of the carbonate ions remains up to 800 °C (0.06). On the other hand, all the carbonates disappeared after reduction at 700 °C, which confirms well the attribution of the TPR band located between 600 and 700 °C.

Table 2
XPS $CO_3^-$/Al ratio for the 0.8/0.2/1/1 HDL before and after calcination (450 and 800 °C), and after reduction at 700 °C

| NiCuMgAl (0.8/0.2/1/1) | $CO_3^-$/Al ratio |
|---|---|
| As-synthesised (HDL) | 0.36 |
| Calcined (450 °C) | 0.07 |
| Calcined (800 °C) | 0.06 |
| Reduced (700 °C) | 0. |

### 3.2. Acid–base character of mixed oxides

We have used two complementary techniques (adsorption microcalorimetry and adsorption XPS) to study the acidic and basic properties of the NiCuMgAl mixed oxides obtained from the calcination (450 °C) of LDHs. Adsorption microcalorimetry is a powerful technique for these characterisations since it gives the concentration and the strength of the acid or basic sites located on the outer and inner surface of the porous catalytic materials. Adsorption XPS mainly informs on the nature and the relative strength of the external surface sites (Lewis and/or Brönsted sites).

The acidic character of catalysts is usually studied by the adsorption of nitrogen basic probes as ammonia or pyridine (or homologue molecules) [19]. Here, we used $NH_3$ which titrates the main part of acid sites because of its small size and its relatively strong basicity. In FTIR, the basic properties are the most often analysed using carbon dioxide as acid probe. However in our case, on the one hand, the carbonate anions which partly remain after calcination prevent the analysis of the XPS C 1s band, and, on the other hand, $CO_2$ is a weak acid which tends to be desorbed in the UHV conditions of the XPS analyses. The adsorption of sulphur dioxide is more suitable to study basicity by XPS [20] because it is a stronger acid probe gas [21] and it displaces a part of the carbonates still present.

As already indicated, we studied the evolution of the basicity and the acidity as a function of the Cu/(Cu + Ni) ratio (with Mg/Al constant) or the Mg/Al ratio (with Cu/(Cu + Ni) constant).

#### 3.2.1. Basicity

Fig. 4 shows the differential heats of adsorption of $SO_2$ versus coverage of the NiCuMgAl mixed oxides with constant Mg/Al (equal to 1) and variable Cu/(Cu + Ni) ratios. As of the first dose, the curves show a plateau characteristic of homogeneous basic sites (in terms of strength) between 150

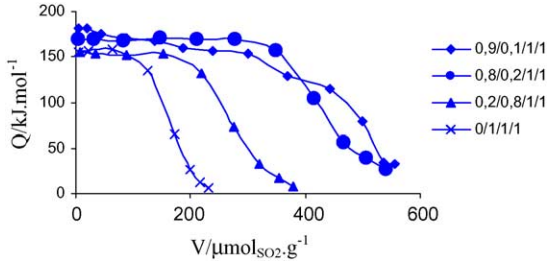


Fig. 4. Differential heats of $SO_2$ adsorption vs. coverage on NiCuMgAl mixed oxides.

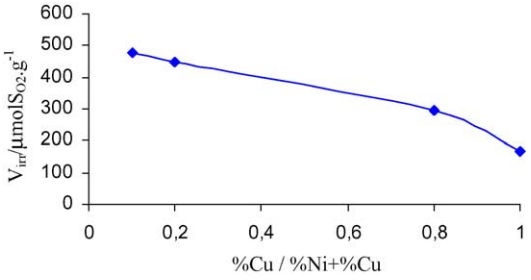


Fig. 5. Irreversibly chemisorbed $SO_2$ vs. Cu/(Ni + Cu) (with constant Mg/Al) on NiCuMgAl mixed oxides.

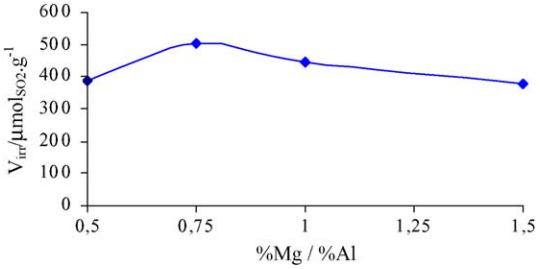


Fig. 7. Irreversibly chemisorbed $SO_2$ vs. Mg/Al ratio (with constant Cu/(Ni + Cu)) on NiCuMgAl mixed oxides.

and 180 kJ mol$^{-1}$. The strength and the number of these sites follow the Ni concentration as shown also in Fig. 5 which reports the amount of $SO_2$ irreversibly adsorbed (proportional to the concentration of the intermediate and strong sites). This is in agreement with the TPR results and the presence of remaining carbonates ions in the Ni-rich oxides. The number of basic sites is also related to the specific surface area (Table 1). The fast decrease of the differential heats of adsorption at the end of the plateau of each curve indicates that the weak sites are very few in these mixed oxides. These characteristics are summarised in Fig. 6 which shows the strength distribution of the basic sites (in terms of chemisorbed $SO_2$ amounts associated with an adsorption heat range). The sites are separated in three categories according to their force defined by the value of differential heats of adsorption: strong ($Q$ > 150 kJ mol$^{-1}$), intermediate ($Q$ between 150 and 100 kJ mol$^{-1}$) and weak ($Q$ < 100 kJ mol$^{-1}$). The Ni-rich samples present a large majority of strong and homogeneous sites (especially 0.8/0.2/1/1), whereas the Cu-rich samples which present smaller surface areas (Table 1) have basicity definitely lower.

The influence of the Mg/Al ratio on the basicity of the mixed oxides is shown in Fig. 7 which reports the $SO_2$ amount irreversibly adsorbed ($V_{irr}$) versus Mg/Al (Cu/(Cu + Ni) ratio was maintained constant and equal to 0.2; we chose this ratio because the previous results showed high basicity for it, thus it could be possible to better evidence the influence of the Mg/Al ratio on this property). The variations are smaller than previously observed, but it seems that a maximum of basicity was obtained for a Mg/Al ratio around 0.75. Taking into account the small variation of basicity when the Mg/Al ratio is modified it could assume that the basicity of our samples is rather determined by the substitution of Mg in brucite layers with other divalent cations, than with trivalent cations.

An example of XPS S 2p peak after adsorption of $SO_2$ at 80 °C on the mixed oxides is reported in Fig. 8. This peak is decomposed into two doublets ($2p^{3/2}$–$2p^{1/2}$) irrespective of the sample composition. The first $2p^{3/2}$ peak appeared at 167.4 eV and the second at 169.2 eV. The first doublet can be assigned to the interaction of $SO_2$ molecules with hydroxyl ($OH^-$) surface groups (Brönsted sites). Indeed, after adsorption of $SO_2$ over CuMgAl LDHs before calcination ($SO_2$ reacts only with the hydroxyl groups), the binding energy S $2p^{3/2}$ is at about 167.2 eV [22]. The second doublet corresponds to $SO_2$ in interaction with $O^{2-}$ anions (∼169 eV) [18], i.e. Lewis sites. The relative proportion of these components (60 and 40% respectively), whatever the composition of the oxides, shows that the main part of the surface basicity is due to the surface OH groups.

### 3.2.2. Acidity

The differential heats of ammonia adsorption on the mixed oxides as a function of the $NH_3$ uptake are reported in Fig. 9. The heats, initially around 140 kJ mol$^{-1}$ (thus indicating an absence of strong sites), decrease to 70 kJ mol$^{-1}$ (chemisorption–physisorption limit) without any plateau, showing a heterogeneity of the strength of the acid sites,

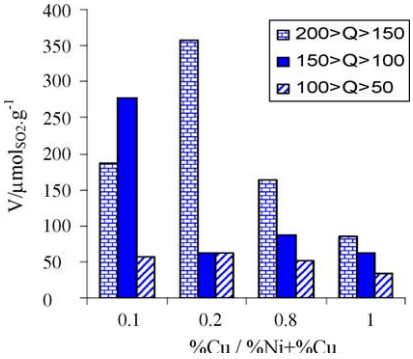


Fig. 6. Repartition of the basic sites vs. strength as a function of Cu proportion (with constant Mg/Al).

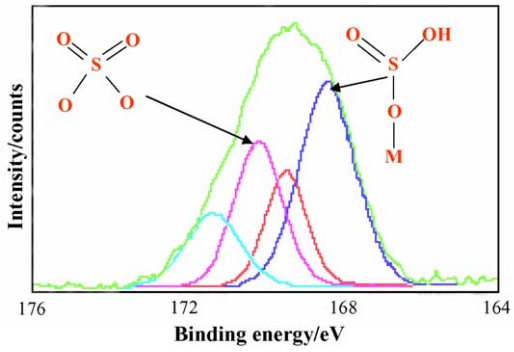


Fig. 8. S 2p XP spectrum after adsorption of $SO_2$ on NiCuMgAl (0.8/0.2/1/1) mixed oxide.

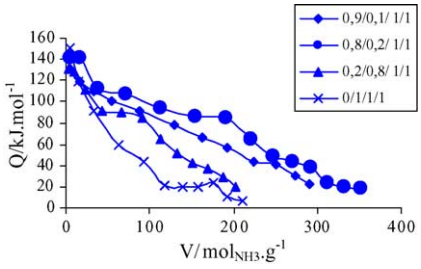


Fig. 9. Differential heats of $NH_3$ adsorption vs. coverage on NiCuMgAl mixed oxides.

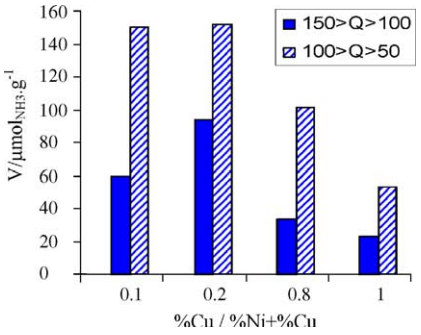


Fig. 10. Repartition of the acid sites vs. strength as a function of Cu proportion (with constant Mg/Al) on NiCuMgAl mixed oxides.

contrary to that of the basic sites. This heterogeneity can be related with the heterogeneity of the interactions between the nickel atoms and the other metallic elements evidenced by the TPR study. These interactions influence the electronic population of the atoms, in particular that of nickel, and therefore modify their acidity. The amount and the repartition of the sites in terms of acid strength (Figs. 9 and 10) indicate a relatively weak acidity for these samples which is however dependant of the Cu/Ni proportions. The overall acidity increases approximately with the ratio Ni/Cu and the concentration of the medium sites reaches a maximum for the composition 0.8/0.2/1/1. The small difference observed between the samples 0.8/0.2/1/1 and 0.9/0.1/1/1 comes probably from the specific surface (316 $m^2\ g^{-1}$ for 0.8/0.2/1/1 and 272 $m^2\ g^{-1}$ for 0.9/0.1/1/1).

Regarding the basicity, the Mg/Al ratio has a slight influence on the acidity. It seems that the maximum of acidity is obtained for a ratio close to the unity (Fig. 11).

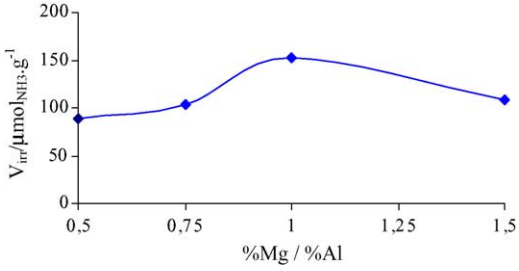


Fig. 11. Irreversibly chemisorbed $NH_3$ amounts vs. Mg/Al ratio (with constant Cu/(Ni + Cu)) on NiCuMgAl mixed oxides.

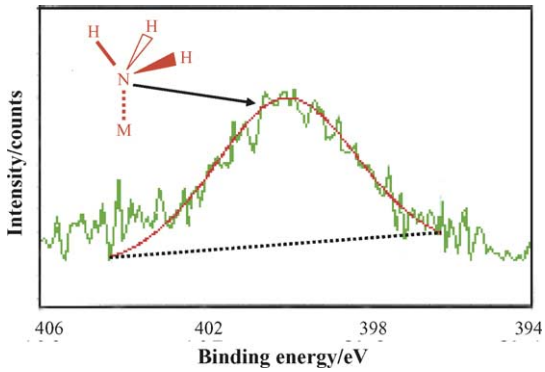


Fig. 12. N 1s XP spectrum after adsorption of $NH_3$ on NiCuMgAl (0.8/0.2/1/1) mixed oxide.

As previously with the $SO_2$ adsorption, XPS analyses after $NH_3$ adsorption allow to identify the nature of acid sites on the solid surface [20]. The neighbourhood of its nitrogen atom is modified differently when the ammonia molecule reacts with a Brönsted or Lewis site. The former leads to the formation of an ammonium ion characterised by a N 1s binding energy higher than 402 eV. The Lewis acid is defined as an acceptor of electronic doublet (corresponding thus to a metal with a vacancy) and the N 1s binding energy for chemisorbed ammonia on this site is lower than 401 eV. In our case, the adsorption of ammonia reveals only the presence of Lewis sites, the N 1s binding energy being about 400 eV (Fig. 12).

## 4. Conclusion

In this work, the thermal evolution of NiCuMgAl layered double hydroxides has been studied, as well as the acid–base properties of the oxides resulting from their calcination at 450 °C. At this temperature, physisorbed, interlayer and dehydroxylation water is released with $CO_2$ coming from the compensation carbonate ions, although some carbonates are still detected by TPR and XPS, blocking a part of the strong basic sites.

The TPR study has evidenced a slight charge transfer from Ni to Cu in the case of Ni-rich oxides and various interactions between Ni and the other elements, in particular $Al_2O_3$. These various interactions induce an heterogeneity of the strength of the acid sites which are all of Lewis type (metallic sites). These sites are rather weak, particularly in the Cu-rich compounds.

Just like the acidity, the basicity of the mixed oxides is more sensible to the Ni/Cu ratio than to the Mg/Al ratio. The $SO_2$ adsorption data indicate an increase of the concentration and the strength of the basic sites with the amount of nickel. The strength of these sites is homogeneous (particularly the composition 0.8/0.2/1/1). The XPS analyses show that about 60% of the surface basic sites are of Brönsted type (OH) and 40% of Lewis type ($O^{2-}$). Indeed the surface of these mixed oxides remains still partly hydroxyled.

Catalytic tests (condensation reactions) are in progress to correlate them to these observations.

## References


[1] F. Cavani, F. Trifirò, A. Vaccari, Catal. Today 11 (1991) 173.
[2] S.M. Auer, S.V. Greding, R.A. Köppel, A. Baiker, J. Mol. Catal. A: Chem. 141 (1999) 193.
[3] D.A. Shirley, Phys. Rev. B 5 (1972) 4709.
[4] G. Forsanari, M. Gazzano, D. Matteuzzi, F. Trifirò, A. Vaccari, Appl. Clay Sci. 10 (1995) 69.
[5] O. Clause, M.G. Coelho, M. Gazzano, D. Matteuzzi, F. Trifirò, A. Vaccari, Appl. Clay Sci. 8 (1993) 169.
[6] I.J. Shannon, F. Rey, G. Sankar, J.M. Thomas, T. Maschmeyer, A.M. Waller, A.E. Palomares, A. Corma, A.J. Dent, G. Neville Greaves, J. Chem. Soc., Faraday Trans. 92 (1996) 4331.
[7] S.M. Auer, S.V. Greding, R.A. Köppel, A. Baiker, J. Mol. Catal. A: Chem. 141 (1999) 193.
[8] M.A. Aramendia, Y. Avilés, V. Borau, J.M. Luque, J.M. Marinas, J.R. Ruiz, F.J. Urbano, J. Mater. Chem. 9 (1999) 1603.
[9] S. Casenave, H. Martinez, C. Guimon, A. Auroux, V. Hulea, A. Cordoneanu, E. Dumitriu, Thermochim. Acta 379 (2001) 85.
[10] S. Casenave, H. Martinez, C. Guimon, A. Auroux, V. Hulea, E. Dumitriu, J. Therm. Anal. Cal. 72 (2003) 191.
[11] V. Rives, S. Kannan, J. Mater. Chem. 10 (2000) 489.
[12] G. Fierro, M. Lo Jacono, M. Inversi, P. Porta, F. Cioci, R. Lavecchia, Appl. Catal. A 137 (1996) 327.
[13] B. Coq, D. Tichit, S. Ribet, J. Catal. 189 (2000) 117.
[14] S.D. Robertson, B.D. McNicol, J.H. De Baas, S.C. Kloet, J.W. Jenkins, J. Catal. 37 (1975) 424.
[15] R. Brown, M.E. Cooper, D.A. Whan, Appl. Catal. 3 (1982) 177.
[16] M. Afzal, C.R. Theochris, S. Karim, Colloid. Polym. Sci. 271 (1993) 1100.
[17] C. Guimon, A. Auroux, E. Romero, A. Monzon, Appl. Catal. A 251 (2003) 199.
[18] V.R. Choudary, A.M. Rajput, J. Catal. 139 (1993) 326.
[19] A. Boreave, A. Auroux, C. Guimon, Micropor. Mater. 11 (1997) 275.
[20] C. Guimon, A. Gervasini, A. Auroux, J. Phys. Chem. B 105 (2001) 10316.
[21] S.M. Auer, S.V. Greding, R.A. Köppel, A. Baiker, J. Mol. Catal. A 141 (1999) 193.
[22] S. Cazenave, H. Martinez, C. Guimon, E. Dumitriu, V. Hulea, Prog. Catal. 10 (2001) 1.